

Mass Spectrometric Imaging of Red Fluorescent Protein in Breast Tumor Xenografts

*Kamila Chughtai¹, Lu Jiang², Harm Post³, Paul T. Winnard Jr.², Tiffany R. Greenwood²,
Venu Raman^{2,4}, Zaver M. Bhujwalla^{2,4}, Ron M.A. Heeren^{1,3} and Kristine Glunde^{2,4}*

¹Biomolecular Imaging MS group, FOM Institute AMOLF, Amsterdam, The Netherlands

²Division of Cancer Imaging Research, The Russell H. Morgan Department of Radiology and Radiological Science, The Johns Hopkins University School of Medicine, Baltimore, MD, USA

³The Netherlands Proteomics Centre, Utrecht, The Netherlands

⁴Sidney Kimmel Comprehensive Cancer Center, The Johns Hopkins University School of Medicine, Baltimore, Maryland, USA

Running title: Multimodal imaging of red fluorescent protein

Corresponding authors/Address reprint requests to:

Kristine Glunde: address, The Russell H. Morgan Department of Radiology and Radiological Science, The Johns Hopkins University School of Medicine, 212 Traylor Building, 720 Rutland Avenue, Baltimore, MD 21205; phone, +1-410-614-2705; fax, +1-410-614-1948; e-mail, kglunde@mri.jhu.edu.

Ron M. A. Heeren: address, FOM Institute AMOLF, Science Park 104, 1098 XG Amsterdam, The Netherlands; phone, +31-20-486 7547100; fax, +31-20-7547290; e-mail, heeren@amolf.nl.

Abstract

Mass spectrometric imaging (MSI) in combination with electrospray mass spectrometry (ESI-MS) is a powerful technique for visualization and identification of a variety of different biomolecules directly from thin tissue sections. As commonly used tools for molecular reporting, fluorescent proteins are molecular reporter tools that have enabled the elucidation of a multitude of biological pathways and processes. To combine these two approaches, we have performed targeted MS analysis and MALDI-MSI visualization of a tdTomato red fluorescent protein, which was expressed exclusively in the hypoxic regions of a breast tumor xenograft model. For the first time, a fluorescent protein has been visualized by both optical microscopy and MALDI-MSI. Visualization of tdTomato by MALDI-MSI directly from breast tumor tissue sections will allow us to simultaneously detect and subsequently identify novel molecules present in hypoxic regions of the tumor. MS and MALDI-MSI of fluorescent proteins, as exemplified in our study, is useful for studies, in which the advantages of MS and MSI will benefit from the combination with molecular approaches that use fluorescent proteins as reporters.

Introduction

Mass spectrometric imaging (MSI) is nowadays a widely used technique for detection and visualization of a variety of different biomolecules directly from thin tissue sections of different origin [1]. MSI is an excellent molecular discovery tool because of its imaging capabilities that cover a broad range of biomolecules of different chemical composition and biological properties, allowing the exploration of complex biological tissue surfaces. In addition, there is no requirement for labeling procedures or *a priori* knowledge about a sample's biochemical composition when performing MSI. MSI easily combines with other imaging techniques, such as optical microscopy, thereby adding additional molecular imaging information to the biological processes under investigation.

The tdTomato protein belongs to the family of fluorescent proteins, which are often used as genetically encoded fusion tags in biomedical applications that utilize cell cultures and animal models [2]. tdTomato is a tandem dimer (td) generated by linking together, via a short random coil sequence, two mutated 28-kDa monomer units of the tetrameric DsRed fluorescent protein [3, 4]. The monomer unit of tdTomato was specifically selected based on its low propensity to aggregate and because it is nontoxic. The generation of the dimer gives the protein an exceptional brightness [2, 5]. Thus, the combination of a high quantum yield of 0.69 with an extinction coefficient per chain of $138,000 \text{ M}^{-1} \text{ cm}^{-1}$, makes tdTomato the brightest of the currently available fluorescent proteins [6]. Additionally, tdTomato retains desirable physical characteristics observed in many of the smaller monomeric fluorescent proteins, such as a relatively short maturation half-time of one hour at 37°C and excellent photostability, all of which make it useful for *in vivo* optical imaging studies [6]. It has been widely used in biomedical studies for the detection of proteins of interest fused to tdTomato as a fluorescent reporter [7], as well as in studies of noninvasive optical tracking of cancer cells *in vivo* [8]. In the latter case, it has been established that its emission is readily

detectable at or above 620 nm, which is outside the range of absorption and autofluorescence of living tissue [8]. Due to these characteristics, along with its brightness, tdTomato can be detected as deep as 1-cm below the tissue surface. These properties facilitate its use in *in vivo* fluorescence imaging studies in real-time in live animal models [8, 9]. Bioimaging that employs tdTomato fluorescent protein as a fluorescent label has multiple benefits over other techniques in which fluorescent dyes or bioluminescence are used [8].

Here our goal was to detect, identify and visualize the tdTomato protein present in human breast tumor xenograft models by using a multimodal imaging approach that merged optical microscopy and MSI combined with bottom-up proteomics. In our study, tdTomato was used to visualize hypoxic tumor regions, which contribute to tumor aggressiveness, in a genetically engineered tumor xenograft model [10]. The ability to detect tdTomato in the hypoxic regions of this breast tumor model with MSI will enable us to use MSI to map biomolecules that are up- or down-regulated in hypoxic tumor regions. Understanding such hypoxia-induced changes in cancer is crucial for developing novel more effective tumor therapies that can target the often chemo- and radio-resistant hypoxic regions in tumors.

Materials and Methods

Chemicals and materials. The MALDI matrix α -cyano-4-hydroxycinnamic acid (CHCA) was purchased from Sigma (Germany), ethanol, acetic acid, water, acetonitrile (ACN), trifluoroacetic acid (TFA) were purchased from Biosolve (The Netherlands). Modified proteomics grade trypsin was purchased from Sigma (Germany) or Promega (USA). Cresyl violet acetate and gelatin Type A were purchased from Sigma (USA).

Mass spectrometric analysis of cell lysates. MDA-MB-231-EF1 α -tdTomato cells [8] were grown under standard cell culture conditions in RPMI medium. MDA-MB-231-EF1 α -tdTomato cells were collected and lysed using ProteaPrep Cell Lysis Kit, Mass Spec Grade (Protea Biosciences, Inc., USA) according to the manufacturer's protocol. Protein concentrations of lysates were determined using the Bio-Rad Protein Assay (BioRad DC, USA, Cat no 500-0116). NATIVE-PAGE (Bio-Rad, USA) was run in Tris/glycine buffer without SDS added. The 8% gel was loaded with 45 μ g of total protein and the red fluorescent band was cut out under a home-built fluorescent lamp equipped with a Gemini 300 high intensity, short arc light source, a 600 to 660 nm emission filter, and a Nikon Coolpix digital camera (Nikon Instruments, Inc, Melville, NY). Gel pieces were frozen at -80°C until further analysis.

MALDI-MS analysis of gel bands: The fluorescent gel bands were sliced into several gel pieces of 1-mm x 1-mm size and 50 μ L of 2:1 ACN:25 mM NH₄HCO₃ was added for 15 min. The supernatant was removed and 50 μ L of 25 mM NH₄HCO₃ was added for 10 min. The last two steps were repeated and followed by a final wash in 2:1 ACN:25 mM NH₄HCO₃ for 15 min. The supernatant was removed and the gel pieces were dried in a speed vacuum centrifuge. Trypsin prepared in 25 mM NH₄HCO₃ at a concentration of 12.5 ng/ μ L was added to the gel pieces and incubated on ice for 20 min. Following incubation, 25 mM NH₄HCO₃ buffer was added to cover the gel pieces, followed by incubation at 37°C for 4.5 hours. Peptides were extracted by first pooling the supernatant into a second tube and adding 50 μ L 2:1 ACN:25 mM NH₄HCO₃ to the gel pieces, followed by 15 min incubation in a shaker at RT. The supernatant was collected and transferred to the tube containing the supernatant from the previous extraction. Then, 100% ACN was added to the gel pieces and the tube was shaken for 20 min at RT. The supernatant was removed and transferred to a tube containing supernatant from the previous extractions. The supernatant was dried down to

approximately 10 μL using a speed vacuum microcentrifuge and then mixed with CHCA matrix prepared at a concentration of 10 mg/mL in 1:1 ACN:H₂O/0.1% TFA. This mixture was spotted on a MALDI target plate for MS analysis with a Q-TOF instrument (Synapt, Waters, UK).

LC-ESI-MS analysis of gel bands: The fluorescent gel bands were cut into small pieces and washed with 250 μL milliQ. After removing milliQ, 100% ACN was added, the gel pieces were vortexed, and ACN was removed. The gel pieces were covered with ACN, vortexed and incubated for 15 min at RT. ACN was removed and 100 μL of 10 mM DTT in 50 mM NH₄HCO₃ was added. Gel pieces were incubated in a shaker for 1 h at 60°C. DTT was removed and samples were cooled to RT. One hundred percent ACN was added to cover the gel pieces, vortexed, removed, and a new portion of ACN was added to cover the gel pieces followed by vortexing and incubation for 15 min at RT. ACN was removed and 100 μL of 54 mM fresh iodoacetamide was added and incubated at RT in the dark for 30 min. Iodoacetamide was removed and 100% ACN was added to cover the gel pieces, vortexed, and removed. This step was performed once more. The following washing procedure was performed twice: 100 μL of 50 mM NH₄HCO₃ was added, vortexed and incubated for 15 mins at RT. After the ammonium bicarbonate was removed, two times 100 μL of 100% ACN was added, vortexed, and removed. Trypsin solution was prepared in 50 mM NH₄HCO₃ at a concentration of 3 ng/ μL and 20 μL of this trypsin solution was added to cover the gel pieces, followed by incubation on ice for 90 min. Excess trypsin was removed and 20 μL of 50 mM NH₄HCO₃ was added, followed by overnight incubation at 37°C. Then, the first supernatant was transferred to a new tube. One hundred microliters 100% ACN were added to the gel pieces, vortexed and incubated for 15 min at RT. This ACN treatment was repeated three times and each time the supernatants were pooled. The pooled supernatant was dried in a vacuum

microcentrifuge and 40 μ L of 10% formic acid was added prior to LC-MS analysis using an LTQ Orbitrap mass spectrometer (Thermo Fisher) equipped with a nanoHPLC system (Agilent).

Breast tumor imaging. The human breast cancer cell line MDA-MB-231 was genetically modified to express tdTomato red fluorescent protein under the control of hypoxia response elements as previously described [11]. Cells in 0.05 mL of Hank's Balanced Salt solution (Sigma) were injected into the upper thoracic mammary fat pad of athymic nude mice (2×10^6 cells/injection) and tumor growth was monitored with standard calipers. When tumors reached a volume of approximately 500-mm^3 , mice were sacrificed and tumors were removed. Each tumor was embedded into a gelatin block prepared using 15-mm x 15-mm x 5-mm cryomolds (Sakura Finetek, USA), 10% gelatin, cooled to 30°C in order to prevent tissue degradation, and three cresyl violet fiducial markers, which were injected inside the gelatin block next to the tumor as previously described [12-14]. This block was sectioned into serial 2-mm thick fresh tumor sections using an acrylic adjustable tissue slicer (12-mm depth up to 25-mm width; Braintree Scientific, Inc, Braintree, MA) and tissue slicer blades (Braintree Scientific, Inc). These serial fresh tumor xenograft sections were each placed on individual microscope slides (Fisherbrand catalog number 12-550-34; Fisher Scientific, Pittsburgh, PA), and stored in an ice-box containing ice on the bottom, with the slides located on a perforated plate at approximately 1-cm above the ice to minimize tissue degradation. Fresh sections were imaged by bright field and fluorescence microscopy with a 1x objective attached to a Nikon inverted microscope, equipped with a filter set for 528 to 553 nm excitation and 600 to 660 nm emission, and a Nikon Coolpix digital camera (Nikon Instruments, Inc, Melville, NY). Bright field microscopy captured the position of the fiducial markers inside the gelatin block as well as the shape of the tumor tissue. The fluorescence of

tdTomato expression in hypoxic regions of these tumor sections was detected by fluorescence microscopy. All 2-mm thick sections were snap frozen immediately after microscopic imaging. From each 2-mm thick section, 10- μ m thick sections were cut at -16°C for MSI using a Microm HM550 cryo-microtome (Microm International GmbH, Walldorf, Germany). A distance of 500- μ m was kept between all 10- μ m thick sections. Tissue sections for MSI analysis were mounted onto 25-mm x 50-mm x 1.1-mm, $R_s=4-8 \Omega$ Indium Tin Oxide (ITO) coated slides (Delta Technologies, USA).

Prior to MSI analysis, tissue sections were briefly washed by immersing them twice in 70% ethanol and dried in a vacuum desiccator for 10 min. Trypsin was resuspended in water at a concentration of 0.05 μ g/ μ L, and 5 nL per spot in a 150- μ m x 150- μ m raster was deposited by a CHIP-1000 piezo electric spotting robot (Shimadzu, Japan). After trypsin deposition, tissue sections were incubated in a humid chamber at 37°C for 12 h. CHCA matrix was prepared at a concentration of 10 mg/mL in 1:1 ACN:H₂O/0.1% TFA and applied by an ImagePrep (Bruker, Germany) application system. Samples were analyzed on a MALDI-Q-TOF (Synapt HDMS, Waters, U.K.) instrument in time-of-flight (TOF) mode detecting positive ions. The images were acquired at a spatial resolution of 150- μ m \times 150- μ m.

Image analysis. Co-localization analysis was performed to quantify the correlation between tdTomato MSI image and the corresponding optical tdTomato fluorescence image. A total of three 10- μ m thick cryo-sections, which were used for MSI, were obtained from the corresponding 2-mm thick fresh tissue section, which were scanned by microscopic imaging. Since the thickness of the tissue sections for MSI is much smaller than that of the sections used to obtain optical bright field and fluorescence images, the MSI images were subjected to a projection operation along the thickness direction of the data. This projection operation

consisted of the following steps: 1) the three MSI images were aligned by the centroid positions of the external fiducial markers; 2) then those three aligned MSI images were summed up to obtain total ion abundance. Since the spatial resolution of an MSI image is also much lower than that of an optical bright field/fluorescence image and the noise level of an MSI image is much higher than that of an optical bright field/fluorescence image, a nonlinear two-dimensional median filtering method was applied to reduce the noise and preserve the tumor edge in the summed-up MSI image. A combined fiducial marker and tumor boundary based image registration method [13, 14] was applied to both the summed-up MSI image and the optical bright field/fluorescence image. The tumor region was masked out by the active shape model in all images [13, 14]. The scattering distribution of the registered MSI ion intensity and optical fluorescence signal were plotted against each other, and the resulting Pearson's correlation coefficient was calculated to investigate the linearity between registered MSI ion image and optical fluorescence image.

Results and Discussion

We have for the first time performed MS bottom-up analysis of the tdTomato fluorescent protein, and have subsequently imaged tdTomato with MSI from a tissue containing tdTomato by means of on-tissue digestion and MSI detection of a tdTomato-specific peptide.

tdTomato protein isolation and MS analysis

In order to simplify the search for the tdTomato protein in our MSI experiments, we wanted to obtain a set of reference peptides that can be retraced in the tissue imaging experiments. To this end, we performed bottom-up mass spectrometry (MS) preceded by liquid chromatography (LC) as a separation step and electrospray ionization (ESI), which we combined with matrix assisted laser desorption/ionization (MALDI) MSI for targeted

identification of our molecule of interest (tdTomato). This approach is advantageous when the identification of molecules of interest directly from tissue sections is difficult due to the high complexity of the sample and ion suppression effects [15]. We isolated tdTomato red fluorescent protein from the MDA-MB-231-EF1 α -tdTomato breast cancer cell line in which tdTomato was constitutively expressed under the strong elongation factor 1 α (EF1 α) promoter [8]. After cell lysis and NATIVE-PAGE electrophoresis, the red fluorescent band was cut out and subjected to in-gel trypsin digestion followed by MALDI-MS as well as LC-ESI-MS analysis. LC-ESI-MS identified 10 peptides with different charge states (z) as shown in Table 1. MALDI-MS analysis identified one tdTomato peptide at the mass to charge ratio (m/z) of 2225.0 with the amino acid sequence LDITSHNEDYTIVEQYER as shown in Figure 1. This MALDI identified peptide was additionally observed by LC-ESI-MS as both doubly and triply charged ions.

Due to the compactness of the β -barrel structure of fluorescent proteins or non-fluorescent OmpA [16] and α -hemolysin [17], these proteins are known to display a relatively high resistance to tryptic cleavage [18, 19]. In-gel tryptic cleavage of cyan fluorescent protein (CFP) protein resulted in a sequence coverage of 50% [19]. Our in-gel digestion method resulted in 26% sequence coverage of the tdTomato protein. ESI ionization enabled the detection of multiple tdTomato peptides with different sequence, length and charge state, while MALDI ionization allowed for the detection of one, singly charged tryptic peptide. We employed this tryptic peptide for the first time to visualize the distribution of a fluorescent protein by MSI.

Microscopic imaging of tdTomato in tumor tissue

A human breast tumor xenograft model expressing tdTomato red fluorescent protein in the hypoxic regions was embedded in a gelatin block containing fiducial markers as previously published [12-14]. The gelatin blocks were sectioned into three 2-mm thick sections for *ex vivo* microscopic visualization of the red fluorescent protein. Figure 2 demonstrates multimodal imaging of the 2-mm section obtained from the tumor centre. The corresponding bright field (Figure 2a) and fluorescence (Figure 2b) images were co-registered based on the position of the fiducial markers (M), which were visible in both bright field and fluorescence images. Figure 2c presents an overlay of the bright field and fluorescence images. Letters “M” indicate the positions of the fiducial markers used for coregistration of both images. The fluorescence image of tdTomato has been changed to black for better visualization of the hypoxic region. Figure 2d shows the false color image of tdTomato fluorescence intensity obtained from the 2-mm tumor section shown in Figure 2b.

Mass spectrometric imaging of tdTomato in a tumor

After microscopic imaging, the gelatin-embedded tumor tissue was frozen and further sectioned into 10- μ m thick sections for MSI. Three 10- μ m thick sections were obtained from the central 2-mm tissue section and used for MSI. The MS-detected fiducial markers were used for alignment of MSI data sets obtained from three 10- μ m thick sections. The detection of the tdTomato tryptic-peptide at m/z 2225.0 was used to localize by MSI the hypoxic regions, in which the tdTomato fluorescent protein was expressed driven by a hypoxia response element (HRE)-containing promoter. Figure 2e presents the false color image of the tdTomato tryptic-peptide distribution at m/z 2225.0 obtained by MSI from three summed-up 10- μ m thick sections. The plot shown in Figure 2f presents the correlation analysis, which was obtained by co-localization analysis of the tdTomato images obtained by fluorescence microscopy *versus* MSI, and which resulted in a relatively high correlation coefficient R^2 of

0.7860. Figure 3 presents an expanded spectrum of the region around the ion at m/z 2225.0 detected from the hypoxic tissue region as shown in red and the normoxic region as shown in blue. The tryptic peptide at m/z 2225.0, which was directly detected only from hypoxic, but not from normoxic tumor regions by MSI, was able to distinguish these two regions.

In the present study, the normoxic regions of a given tumor tissue section are considered the negative control because they do not express the red fluorescent tdTomato protein. In comparison, the hypoxic regions from the same tumor section express tdTomato. To exclude the possibility of a potential endogenous signal at m/z 2225.0, a series of experiments on trypsin-digested tumor sections *versus* non-digested sections was performed. In the case of the non-digested sections, no signal with a signal-to-noise $S/N > 1$ was detected at m/z 2225.0.

Our proof-of-principle study demonstrated that MSI can be used in molecular studies in which the expression of a fluorescent protein needs to be mapped in tissue sections. MSI visualization of tdTomato directly from breast tumor tissue sections will allow us in the future to simultaneously detect the hypoxic regions and a multitude of different biomolecules in this tumor xenograft model. With this approach, we will be able to identify biomolecules that are up- or down-regulated in these hypoxic tumor regions.

Conclusions

This study highlights the benefits of multimodal molecular imaging of a breast tumor xenograft model. We have for the first time detected the tdTomato fluorescent protein by bottom-up MS analysis. Subsequently, we have imaged a tryptic peptide from tdTomato by MSI in tumor sections, in which tdTomato was expressed in hypoxic tumor regions of a breast tumor xenograft model genetically modified to express tdTomato under hypoxic

conditions. MSI can provide biochemical information about the heterogeneous composition of the tumor tissue. The fusion of MSI with other *in vivo* or *ex vivo* imaging techniques can offer simultaneous detection and identification of multiple biomolecules of interest such as drugs, lipids, peptides and proteins, directly from a specific region of a thin tissue section.

Acknowledgements

This work is part of the research program of the “Foundation for Fundamental Research on Matter (FOM)”, which is financially supported by the “The Netherlands Organization for Scientific Research (NWO)”. We gratefully acknowledge financial support from NIH grant R01 CA134695. The authors also gratefully acknowledge continued support from the Netherlands Proteomics Centre (NPC). We are indebted to A.F. Maarten Altelaar and Albert J.R. Heck for enabling LC-ESI-MS/MS experiments in the NPC facility.

References

1. Chughtai, K.; Heeren, R. M. Mass spectrometric imaging for biomedical tissue analysis. *Chem Rev.* **2010**, 110, 3237-3277.
2. Campbell, R. E.; Tour, O.; Palmer, A. E.; Steinbach, P. A.; Baird, G. S.; Zacharias, D. A.; Tsien, R. Y. A monomeric red fluorescent protein. *Proc Natl Acad Sci U S A.* **2002**, 99, 7877-7882.
3. Matz, M. V.; Fradkov, A. F.; Labas, Y. A.; Savitsky, A. P.; Zaraisky, A. G.; Markelov, M. L.; Lukyanov, S. A. Fluorescent proteins from nonbioluminescent Anthozoa species. *Nat Biotechnol.* **1999**, 17, 969-973.
4. Gross, L. A.; Baird, G. S.; Hoffman, R. C.; Baldrige, K. K.; Tsien, R. Y. The structure of the chromophore within DsRed, a red fluorescent protein from coral. *Proc Natl Acad Sci U S A.* **2000**, 97, 11990-11995.
5. Baird, G. S.; Zacharias, D. A.; Tsien, R. Y. Biochemistry, mutagenesis, and oligomerization of DsRed, a red fluorescent protein from coral. *Proc Natl Acad Sci U S A.* **2000**, 97, 11984-11989.
6. Shaner, N. C.; Campbell, R. E.; Steinbach, P. A.; Giepmans, B. N.; Palmer, A. E.; Tsien, R. Y. Improved monomeric red, orange and yellow fluorescent proteins derived from *Discosoma* sp. red fluorescent protein. *Nat Biotechnol.* **2004**, 22, 1567-1572.
7. Morris, L. M.; Klanke, C. A.; Lang, S. A.; Lim, F. Y.; Crombleholme, T. M. TdTomato and EGFP identification in histological sections: insight and alternatives. *Biotech Histochem.* **2010**, 85, 379-387.
8. Winnard, P. T., Jr.; Kluth, J. B.; Raman, V. Noninvasive optical tracking of red fluorescent protein-expressing cancer cells in a model of metastatic breast cancer. *Neoplasia.* **2006**, 8, 796-806.
9. Deliolanis, N. C.; Kasmieh, R.; Wurdinger, T.; Tannous, B. A.; Shah, K.; Ntziachristos, V. Performance of the red-shifted fluorescent proteins in deep-tissue molecular imaging applications. *J Biomed Opt.* **2008**, 13, 044008.
10. Raman, V.; Artemov, D.; Pathak, A. P.; Winnard, P. T., Jr.; McNutt, S.; Yudina, A.; Bogdanov, A., Jr.; Bhujwalla, Z. M. Characterizing vascular parameters in hypoxic regions: a combined magnetic resonance and optical imaging study of a human prostate cancer model. *Cancer Res.* **2006**, 66, 9929-9936.
11. Krishnamachary, B.; Penet, M. F.; Nimmagadda, S.; Mironchik, Y.; Raman, V.; Solaiyappan, M.; Semenza, G. L.; Pomper, M. G.; Bhujwalla, Z. M. Hypoxia regulates CD44 and its variant isoforms through HIF-1 α in triple negative breast cancer. *PLoS ONE.* **2012 in press.**
12. Chughtai, K.; Jiang, L.; Greenwood, T. R.; Klinkert, I.; Amstalden van Hove, E. R.; Heeren, R. M.; Glunde, K. Fiducial markers for combined 3-dimensional mass spectrometric and optical tissue imaging. *Anal Chem.* **2012**, 84, 1817-1823.
13. Jiang, L.; Greenwood, T. R.; Artemov, D.; Raman, V.; Winnard Jr., P. T.; Heeren, R. M.; Bhujwalla, Z. M.; Glunde, K. Localized Hypoxia Results in Spatially Heterogeneous Metabolic Signatures in Breast Tumor Models. *Neoplasia.* **2012 (in press).**
14. Jiang, L.; Greenwood, T. R.; Amstalden van Hove, E. R.; Chughtai, K.; Raman, V.; Winnard Jr., P. T.; Heeren, R. M. A.; Artemov, D.; Glunde, K. Combined magnetic resonance, fluorescence, and histology imaging strategy in a human breast tumor xenograft model. *NMR Biomed.* **2012 (in press).**

15. Stoeckli, M.; Staab, D.; Schweitzer, A. Compound and metabolite distribution measured by MALDI mass spectrometric imaging in whole-body tissue sections. *International Journal of Mass Spectrometry*. **2007**, 260, 195-202.
16. Surrey, T.; Jahnig, F. Refolding and oriented insertion of a membrane protein into a lipid bilayer. *Proc Natl Acad Sci U S A*. **1992**, 89, 7457-7461.
17. Cheley, S.; Malghani, M. S.; Song, L.; Hobaugh, M.; Gouaux, J. E.; Yang, J.; Bayley, H. Spontaneous oligomerization of a staphylococcal alpha-hemolysin conformationally constrained by removal of residues that form the transmembrane beta-barrel. *Protein Eng*. **1997**, 10, 1433-1443.
18. Chiang, C. F.; Okou, D. T.; Griffin, T. B.; Verret, C. R.; Williams, M. N. Green fluorescent protein rendered susceptible to proteolysis: positions for protease-sensitive insertions. *Arch Biochem Biophys*. **2001**, 394, 229-235.
19. Alvarez, L. A.; Merola, F.; Erard, M.; Rusconi, F. Mass spectrometry-based structural dissection of fluorescent proteins. *Biochemistry*. **2009**, 48, 3810-3812.

Tables

Table 1. LC-ESI-MS and MALDI-MS analyses of tdTomato containing gel pieces.

| Ionization method | Exp m/z^a | Exp MW ^b | Calc MW ^c | delta ^d | z^e | mc ^f | Sequence and modifications |
|-------------------|-------------|---------------------|----------------------|--------------------|-------|-----------------|------------------------------|
| ESI | 462.7439 | 923.4732 | 923.4753 | -0.002 | 2 | 0 | LSFPEGFK |
| ESI | 526.7907 | 1051.567 | 1051.57 | -0.0034 | 2 | 1 | KLSFPEGFK |
| ESI | 351.5302 | 1051.569 | 1051.57 | -0.0015 | 3 | 1 | KLSFPEGFK |
| ESI | 528.2592 | 1054.504 | 1054.508 | -0.0045 | 2 | 0 | HPADIPDYK |
| ESI | 582.7858 | 1163.557 | 1163.561 | -0.0041 | 2 | 0 | DGGHYLVEFK |
| ESI | 388.8599 | 1163.558 | 1163.561 | -0.0033 | 3 | 0 | DGGHYLVEFK |
| ESI | 584.2564 | 1166.498 | 1166.503 | -0.0043 | 2 | 0 | TMGWEASTER |
| ESI | 592.2539 | 1182.493 | 1182.498 | -0.0044 | 2 | 0 | TMGWEASTER Oxidation (M) |
| ESI | 592.3061 | 1182.598 | 1182.603 | -0.0057 | 2 | 1 | HPADIPDYKK |
| ESI | 395.2079 | 1182.602 | 1182.603 | -0.0015 | 3 | 1 | HPADIPDYKK |
| ESI | 648.3034 | 1294.592 | 1294.598 | -0.0053 | 2 | 1 | KTMGWEASTER |
| ESI | 432.5382 | 1294.593 | 1294.598 | -0.0048 | 3 | 1 | KTMGWEASTER |
| ESI | 656.3015 | 1310.588 | 1310.593 | -0.0041 | 2 | 1 | KTMGWEASTER Oxidation (M) |
| ESI | 437.8701 | 1310.588 | 1310.593 | -0.004 | 3 | 1 | KTMGWEASTER Oxidation (M) |
| ESI | 465.9047 | 1394.692 | 1394.698 | -0.0059 | 3 | 1 | LSFPEGFKWER |
| ESI | 469.2523 | 1404.735 | 1404.74 | -0.0049 | 3 | 1 | LKDGGHYLVEFK |
| ESI | 703.376 | 1404.738 | 1404.74 | -0.0026 | 2 | 1 | LKDGGHYLVEFK |
| ESI | 1113.019 | 2224.023 | 2224.028 | -0.0058 | 2 | 0 | LDITSHNEDYTIVEQYER |
| ESI | 742.3483 | 2224.023 | 2224.028 | -0.0054 | 3 | 0 | LDITSHNEDYTIVEQYER |
| MALDI | 2225.01 | 2224.01 | 2224.028 | -0.0827 | 1 | 0 | LDITSHNEDYTIVEQYER |

^aExp m/z – experimental m/z , ^bExp MW – experimental molecular weight, ^cCalc MW – calculated molecular weight, ^ddelta- difference between Exp m/z and Calc MW, ^e z – charge state, ^fmc – miscleavage

Figure legends

Figure 1. MALDI-MS fragmentation of the peptide $[M+H]^+$ at m/z 2225.0 from an in-gel digested 1D native gel band, which was identified as tdTomato peptide with the sequence LDITSHNEDYTIVEQYER.

Figure 2. Multimodal imaging of tdTomato protein expressed in the hypoxic regions of the MDA-MB-231-HRE-tdTomato breast tumor xenograft. (a) Bright field microscopy of 2-mm tumor section obtained for visualizing tumor boundary. The tissue boundary is outlined by a dashed line. (b) Imaging of the hypoxic tumor regions expressing a red fluorescent protein tdTomato by fluorescence microscopy directly from the 2-mm tumor section. (c) Overlay of images acquired by bright field and fluorescence microscopy. Letters “M” indicate positions of fiducial markers used for coregistration of both images. The fluorescent image of tdTomato has been changed to black for better visualization of the hypoxic region. (d) False color image of tdTomato expression obtained from the 2-mm tumor section shown in (b). (e) False color image of tdTomato peptide $[M+H]^+$ at m/z 2225.0 detected from three 10- μ m sections obtained from the 2-mm tumor section shown in (a). (f) Correlation analysis plot resulting from the co-localization analysis of tdTomato images obtained by fluorescence microscopy (d) and MSI (e). The correlation coefficient R^2 was equal to 0.7860. Scale bar, 5-mm.

Figure 3. Spectrum of ions detected during a region-of-interest (ROI) analysis of the MSI data from a MDA-MB-231-HRE-tdTomato tumor section. The ROI-spectrum related to a hypoxic tumor region is shown in red with a peak at m/z 2225.0 (tdTomato tryptic peptide)

indicated by an arrow. The spectrum recorded from a similarly sized ROI in a normoxic tumor region is shown in blue.

Figures

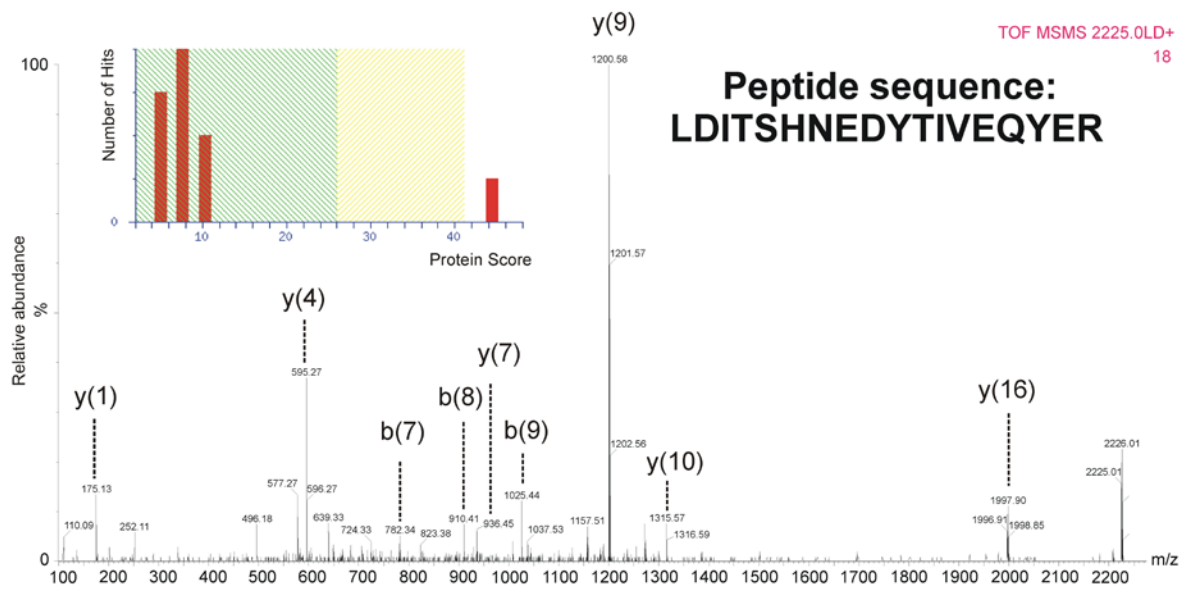


Figure 1.

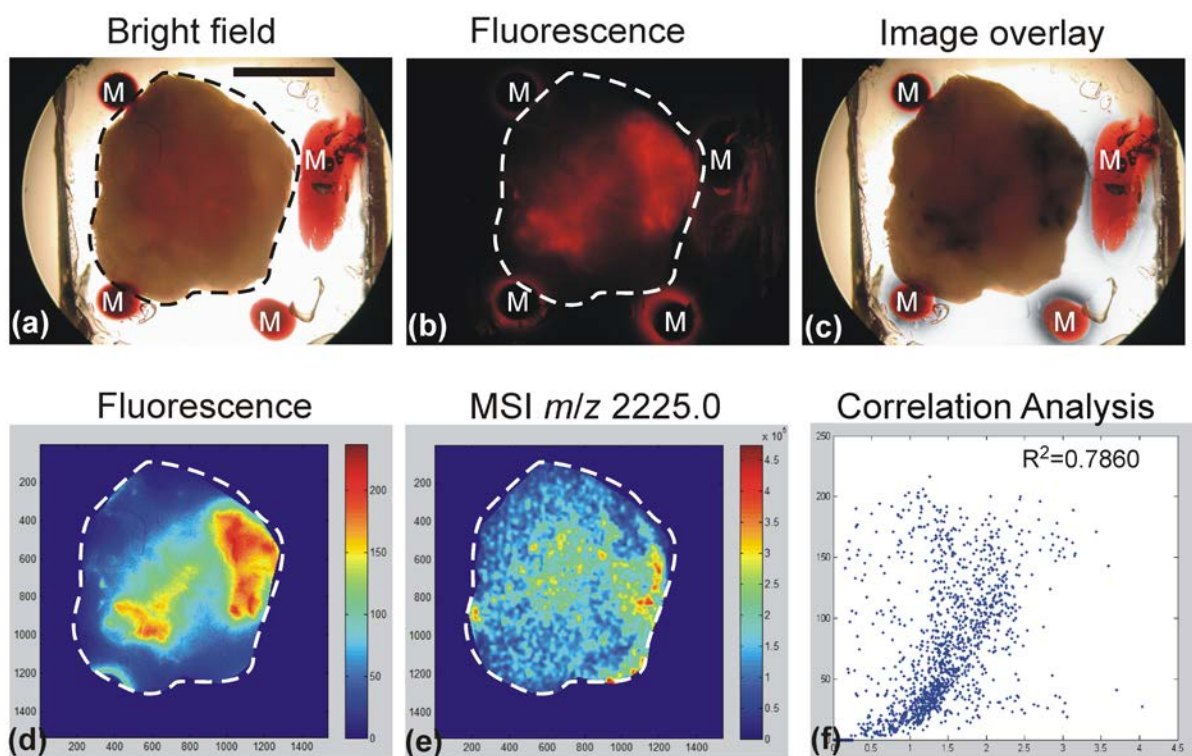


Figure 2.

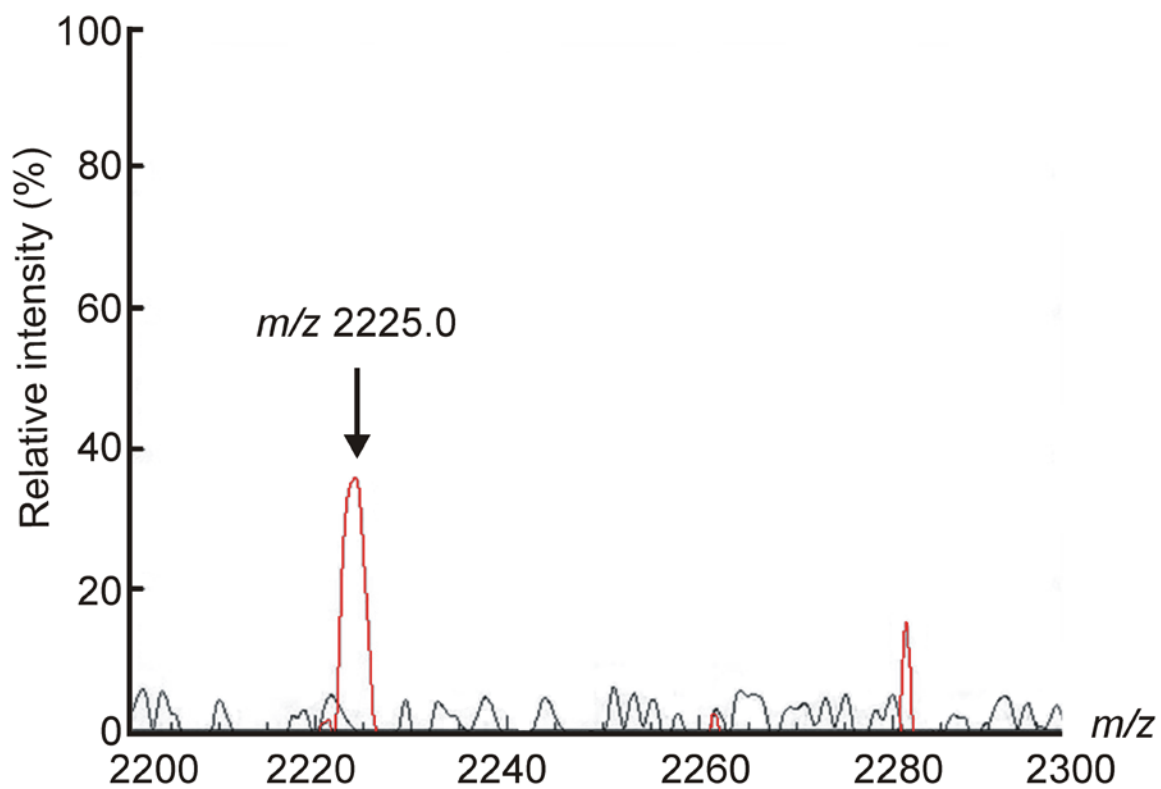


Figure 3.